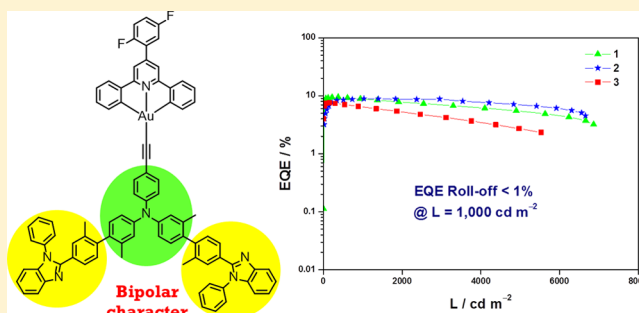


# Bipolar Gold(III) Complexes for Solution-Processable Organic Light-Emitting Devices with a Small Efficiency Roll-Off

Man-Chung Tang, Daniel Ping-Kuen Tsang, Yi-Chun Wong, Mei-Yee Chan,\* Keith Man-Chung Wong,<sup>†</sup> and Vivian Wing-Wah Yam\*

Department of Chemistry, The University of Hong Kong, Pokfulam Road, Pokfulam, Hong Kong

**ABSTRACT:** A new class of bipolar alkynylgold(III) complexes containing triphenylamine and benzimidazole moieties has been synthesized, characterized, and applied as phosphorescent dopants in the fabrication of solution-processable organic light-emitting devices (OLEDs). The incorporation of methyl groups in the central phenyl unit has been found to rigidify the molecule to reduce nonradiative decay, yielding a high photoluminescence quantum yield of up to 75% in spin-coated thin films. In addition, the realization of highly efficient solution-processable OLEDs with an extremely small external quantum efficiency (EQE) roll-off has been demonstrated. At practical brightness level of 1000 cd m<sup>-2</sup>, the optimized devices exhibited a high EQE of up to 10.0% and an extremely small roll-off of less than 1%.



## INTRODUCTION

Encouraging progress on the design and synthesis of highly luminescent phosphorescent metal complexes as well as smart device architecture has boosted the external quantum efficiency (EQE) up to its theoretical limit of 30%.<sup>1</sup> However, severe efficiency roll-off at a luminance required for the application as practical light sources still remains a major challenge to satisfy demanding needs for commercial products. Specifically, a practical lighting system needs to work at a brightness level of 5000 cd m<sup>-2</sup>; on the other hand, the OLED efficiencies drop more than 1 order of magnitude at such high brightness levels.<sup>2,3</sup> Triplet–triplet (T-T) annihilation is the primary energy dissipative process of triplet excitons and is the principal cause of this roll-off.<sup>3</sup> It is found that T-T annihilation is proportional to the square of triplet exciton density within the emissive layer.<sup>4</sup>

Various strategies have been attempted to overcome the efficiency roll-off issue, such as the design of phosphorescent emitters with shorter lifetime,<sup>5</sup> introduction of large dendrons into phosphorescent complexes,<sup>6</sup> or employment of a graded emissive layer to broaden the recombination zone.<sup>7</sup> An area of particular interest involves the development of bipolar materials, where electron-rich and electron-deficient moieties are incorporated into a single molecule. This approach combines the advantages of both functional units to tune the emission color, as well as to have more balanced hole- and electron-transport properties.<sup>7c</sup> Indeed, bipolar host materials have been extensively studied.<sup>8</sup> Su and co-workers reported the synthesis of bipolar host, 2,7-bis(diphenylphosphine oxide)-9-(9-phenylcarbazol-3-yl)-9-phenylfluorene, for blue-emitting iridium(III) bis[(4,6-difluorophenyl)pyridinato-*N,C*2']-picolate (FIrpic).<sup>8b</sup> The optimized device exhibited a

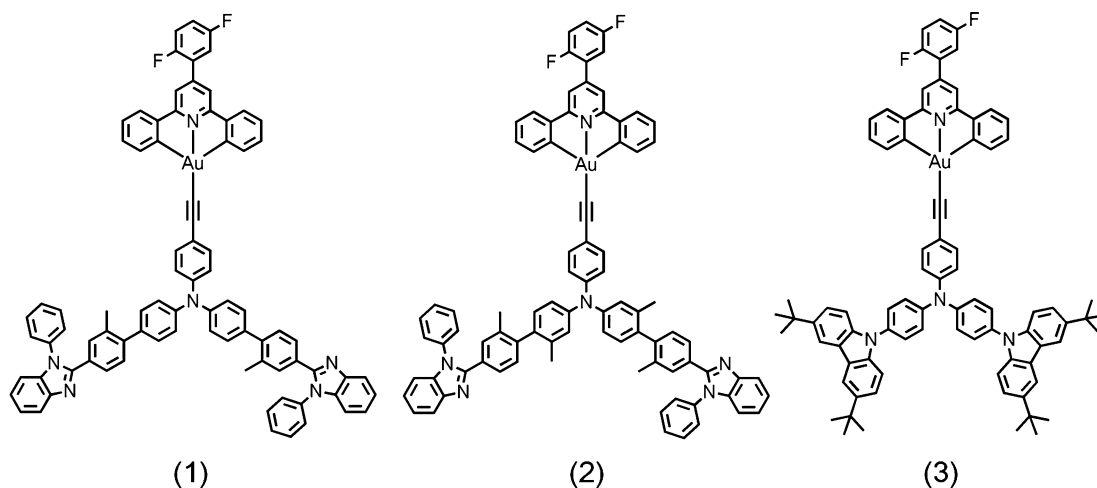
maximum EQE of 14.8% and a current efficiency of 30.8 cd A<sup>-1</sup>. Even at a high brightness of 1000 cd m<sup>-2</sup>, the EQE and current efficiency remained at 13.0% and 26.9 cd A<sup>-1</sup>, respectively. Recently, Kido and co-workers demonstrated a novel bipolar host material, 2,6-bis(3-(carbazol-9-yl) phenyl)pyridine, for FIrpic-based PHOLEDs.<sup>8c</sup> Such device demonstrated a peak EQE of 24.3% and an extremely small roll-off of <7% at a practical brightness of 1,000 cd m<sup>-2</sup>. Meanwhile, a solution-processable bipolar host based on triphenylamine-benzimidazole unit has been reported, in which one or two methyl substituents at the *ortho*-positions of the central biphenyl linkage can twist the molecule and weaken the electronic interactions to reduce molecular aggregation.<sup>8f</sup> Promising iridium(III)-based PHOLEDs have also been successfully fabricated by utilizing bipolar host materials to generate excellent EQE of 25.1% for blue,<sup>8g</sup> 26.9% for green,<sup>8c</sup> 21.6% for red,<sup>8h</sup> and 19.1% for white light emission.<sup>8d</sup>

On the other hand, the development of bipolar phosphors with excellent carrier-transporting properties has been less explored.<sup>9</sup> Although device fabrication processes can be greatly simplified by using commercially available host materials, challenges related to the difficulty in incorporating bipolar ligands into metal centers are yet to be overcome, especially for non-iridium(III) based systems. Meanwhile, the enrichment of the luminescence behavior of organogold(III) complexes has been reported in recent years.<sup>10</sup> In principle, the introduction of strong  $\sigma$ -donating ligands to replace the weak-field chloro ligand in the chlorogold(III) precursor complexes could enlarge the d–d ligand field splitting, resulting in an enhancement of

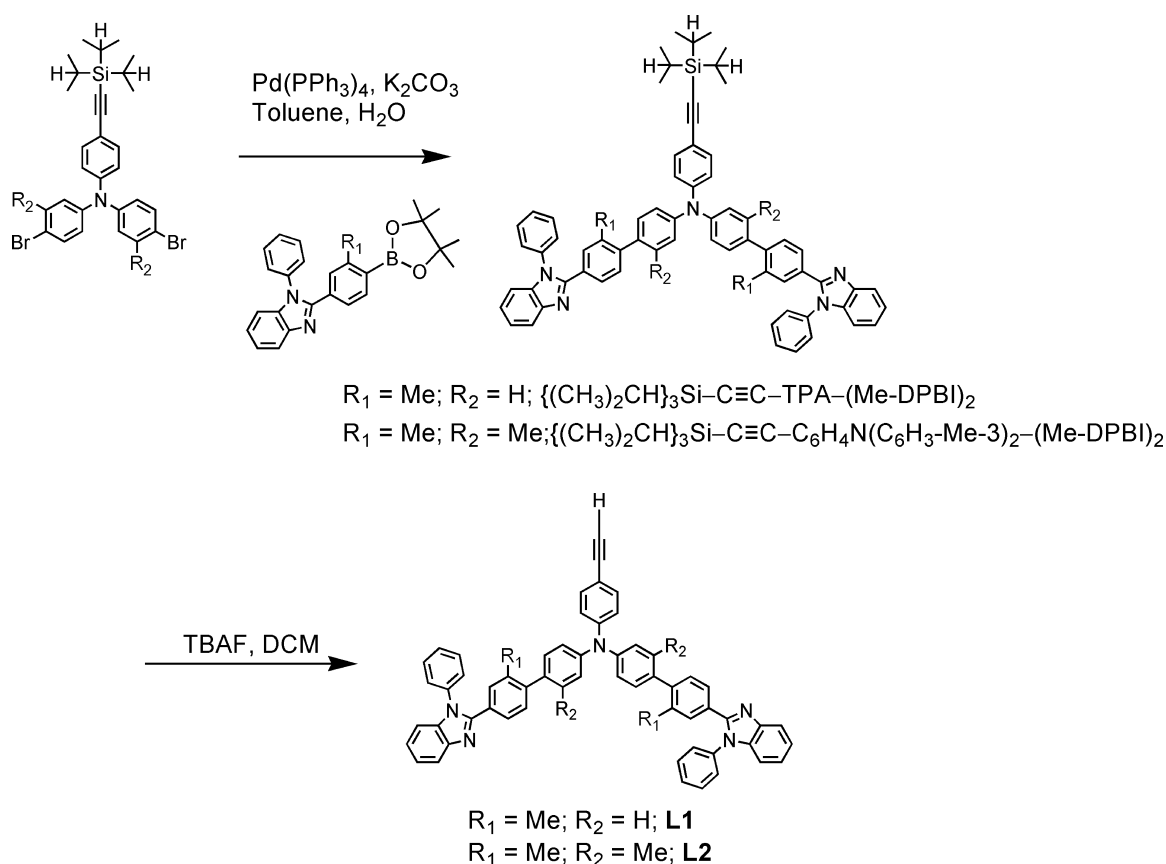
Received: October 16, 2014

Published: December 11, 2014

Scheme 1. Chemical Structures of Alkynylgold(III) Complexes 1–3



Scheme 2. Synthetic Routes of Bipolar Alkynyl Ligands



luminescence of this class of complexes.<sup>10</sup> In addition, our research group recently demonstrated a new class of phosphorescent carbazole-based dendritic alkynylgold(III) complexes and their application studies in the fabrication of PHOLEDs.<sup>10b</sup> Such solution-processable device exhibited a maximum EQE of 7.8% and current efficiency of 24.0 cd A<sup>-1</sup>. The EQE has recently been boosted to 10.1% by changing the solution matrix from chloroform to toluene in the spin-coating process. Here, we take advantage of the dendritic structure to incorporate an electron-accepting benzimidazole moiety featuring a new class of bipolar alkynylgold(III) complexes (Scheme 1). It is found that the introduction of a methyl group

can weaken the  $\pi$ -conjugation between donor and acceptor pairs and rigidify the molecular structure, yielding a high photoluminescence quantum yield (PLQY) of up to 75%. In addition, highly efficient solution-processable PHOLEDs with high EQE of up to 10.0% and current efficiency of 33.6 cd A<sup>-1</sup> have been achieved. More importantly, the EQE of the optimized device doped with 20% complex **2** remains as high as 8.8% and 7.0% at practical brightness levels of 1000 and 5000 cd m<sup>-2</sup>, respectively. These correspond to an extremely small efficiency roll-off of 1% and 21%, respectively.

## RESULTS AND DISCUSSION

**Synthesis and Characterization.**  $\{(\text{CH}_3)_2\text{CH}\}_3\text{Si}-\text{C}\equiv\text{C}-\text{TPA}-(\text{Me}-\text{DPBI})_2$  and  $\{(\text{CH}_3)_2\text{CH}\}_3\text{Si}-\text{C}\equiv\text{C}-\text{C}_6\text{H}_4\text{N}-(\text{C}_6\text{H}_3\text{Me}-3)_2-(\text{Me}-\text{DPBI})_2$  were synthesized by the Suzuki coupling reaction of  $\{(\text{CH}_3)_2\text{CH}\}_3\text{Si}-\text{C}\equiv\text{C}-\text{C}_6\text{H}_4\text{N}(\text{C}_6\text{H}_4\text{Br}-4)_2$  and  $\{(\text{CH}_3)_2\text{CH}\}_3\text{Si}-\text{C}\equiv\text{C}-\text{C}_6\text{H}_4\text{N}(\text{C}_6\text{H}_3\text{Me}-3-\text{Br}-4)_2$  with 4-(1-phenyl-1*H*-benzimidazol-2-yl) phenylboronic acid and 2-methyl-4-(1-phenyl-1*H*-benzimidazol-2-yl) phenylboronic acid, respectively, where TPA, Me-DPBI,  $\{(\text{CH}_3)_2\text{CH}\}_3\text{Si}-\text{C}\equiv\text{C}-\text{C}_6\text{H}_4\text{N}(\text{C}_6\text{H}_4\text{Br}-4)_2$ , and  $\{(\text{CH}_3)_2\text{CH}\}_3\text{Si}-\text{C}\equiv\text{C}-\text{C}_6\text{H}_4\text{N}(\text{C}_6\text{H}_3\text{Me}-3-\text{Br}-4)_2$  represent triphenylamine, 2-(3-methylphenyl)-1-phenyl-1*H*-benzimidazole, *N,N*-bis(4-bromophenyl)-4-[2-[triisopropylsilyl]ethynyl]benzenamine, and *N,N*-bis(4-bromo-3-methylphenyl)-4-[2-[triisopropylsilyl]ethynyl]benzenamine, respectively.<sup>11</sup> **L1** and **L2** were then obtained by deprotection of  $\{(\text{CH}_3)_2\text{CH}\}_3\text{Si}-\text{C}\equiv\text{C}-\text{TPA}-(\text{Me}-\text{DPBI})_2$  and  $\{(\text{CH}_3)_2\text{CH}\}_3\text{Si}-\text{C}\equiv\text{C}-\text{C}_6\text{H}_4\text{N}(\text{Me}-\text{C}_6\text{H}_3\text{Me}-3)_2-(\text{Me}-\text{DPBI})_2$  in 1.0 M tetra-*n*-butylammonium fluoride in THF.<sup>12</sup> The synthetic route of **L1** and **L2** is shown in Scheme 2. 2,6-Diphenyl-4-(2,5-difluorophenyl)pyridine (2,5- $\text{F}_2\text{C}_6\text{H}_3-\text{C}^{\wedge}\text{N}^{\wedge}\text{C}$ )<sup>13</sup> and the chlorogold(III) precursor,  $[\text{Au}\{2,5-\text{F}_2\text{C}_6\text{H}_3-\text{C}^{\wedge}\text{N}^{\wedge}\text{C}\}\text{Cl}]$ ,<sup>14</sup> were prepared by slight modifications of the literature procedures. The incorporation of alkynyl ligand into cyclometalated gold(III) moiety to yield bipolar complexes **1** and **2** was achieved by reacting the corresponding alkynes with the chlorogold(III) precursor in the presence of a catalytic amount of copper(I) iodide in triethylamine and dichloromethane.<sup>10c-g</sup> The synthetic route of complex **3** had recently been communicated.<sup>10b,d</sup> Both complexes are found to be air-stable and thermal-stable. The incorporation of alkynyl ligand into the gold(III) center not only enhances the luminescence behavior but also renders the products soluble in common organic solvents. The identities of complexes **1** and **2** have been confirmed by <sup>1</sup>H NMR spectroscopy, FAB-mass spectrometry, IR spectroscopy, and satisfactory elemental analyses. These new bipolar complexes have been isolated as thermally stable yellow solids with decomposition temperatures ( $T_d$ ) above 300 °C, where  $T_d$  is defined as the temperature at which the material showed a 5% weight loss. The IR spectra of the complexes feature a weak band at 2144–2148  $\text{cm}^{-1}$ , corresponding to the  $\nu(\text{C}\equiv\text{C})$  stretching frequency.

**Photophysical Properties.** The UV–vis absorption and emission spectra of **1** and **2** in dichloromethane at 298 K are shown in Figures 1 and 2, respectively. For comparison, the UV–vis and emission spectra of our previously reported carbazole-based alkynylgold(III) complex **3** are also included.<sup>10b</sup> All complexes show intense vibronic-structured absorption bands at 250–350 nm with a moderately intense

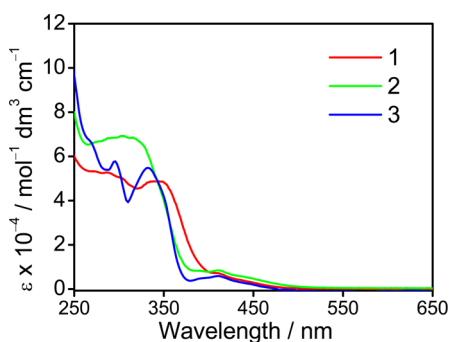


Figure 1. UV–vis absorption spectra of **1–3** in  $\text{CH}_2\text{Cl}_2$  at 298 K.

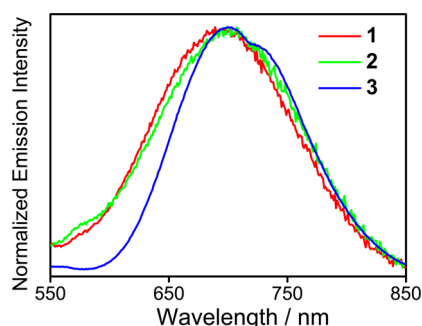
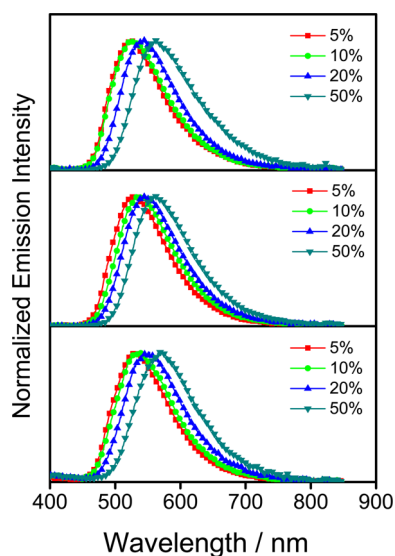


Figure 2. Emission spectra of complexes **1–3** in degassed  $\text{CH}_2\text{Cl}_2$  at 298 K.

vibronic-structured band at ca. 390–410 nm and an absorption tail at 430–500 nm. For complex **1**, the absorption bands at wavelength ( $\lambda$ )  $\leq$  310 nm are mainly attributed to spin-allowed intraligand (IL)  $\pi \rightarrow \pi^*$  transitions of the triphenylamine units, while the absorption shoulder at around 350 nm could be assigned as  $\pi \rightarrow \pi^*$  transitions from the electron-donating triphenylamine moiety to the electron-accepting benzimidazole moiety.<sup>8f</sup> Interestingly, only one absorption band is observed in the high energy region for complex **2**. It could be due to the introduction of the methyl group, which would further weaken the  $\pi$ -conjugation between donor–acceptor pairs and cause a blue shift in energy.<sup>8f</sup> On the other hand, the high-energy absorption bands of complex **3** are attributed to IL  $\pi \rightarrow \pi^*$  transitions of the carbazole units.<sup>15</sup> Meanwhile, a less intense absorption band at ca. 390–410 nm has been observed for all complexes, which is tentatively assigned to a metal-perturbed IL  $\pi \rightarrow \pi^*$  transition of the cyclometalated 2,5- $\text{F}_2\text{C}_6\text{H}_3-\text{C}^{\wedge}\text{N}^{\wedge}\text{C}$  ligand, probably with mixing of a charge transfer character from the aryl ring to the pyridine unit.<sup>10</sup> The absorption tail beyond 430 nm could be assigned as an admixture of IL  $\pi \rightarrow \pi^*$  transitions of the 2,5- $\text{F}_2\text{C}_6\text{H}_3-\text{C}^{\wedge}\text{N}^{\wedge}\text{C}$  and alkynyltriarylamine ligands and ligand-to-ligand charge transfer (LLCT)  $\pi$ -[alkynyltriarylamine]  $\rightarrow \pi^*$ [2,5- $\text{F}_2\text{C}_6\text{H}_3-\text{C}^{\wedge}\text{N}^{\wedge}\text{C}$ ] transitions.<sup>10b-j</sup> Upon excitation at  $\lambda \geq$  380 nm in dichloromethane solution at 298 K, the emission energies of **1–3** are found to be independent of the alkynyl ligands. A broad structureless emission band with maximum at ca. 696 nm has been observed for all complexes (Figure 2). This emission band has been tentatively assigned as derived from an excited state of <sup>3</sup>LLCT  $\pi$ [alkynyltriarylamine]  $\rightarrow \pi^*$ [2,5- $\text{F}_2\text{C}_6\text{H}_3-\text{C}^{\wedge}\text{N}^{\wedge}\text{C}$ ] origin. In the solid-state thin films, **1–3** also display low-energy structureless emission bands. The emission energies are found to shift from 520 to 570 nm in the concentration range of 5–50 wt % in *N,N'*-dicarbazolyl-3,5-benzene (MCP) thin films (Figure 3). Such red emission bands may be due to the excimeric emission arising from the  $\pi$ - $\pi$  stacking of the 2,5- $\text{F}_2\text{C}_6\text{H}_3-\text{C}^{\wedge}\text{N}^{\wedge}\text{C}$  ligand in the solid-state thin films. A similar observation has been reported in other square-planar metal complexes.<sup>10b-h,11,14</sup> Table 1 summarizes the photophysical properties of **1–3**. It should be highlighted that the replacement of the carbazole group in **3** by benzimidazole moieties in **1** and **2** can significantly increase the PLQY. Figure 4 shows the PLQY of complexes **1–3** in MCP thin films. Apparently, the PLQY of thin films doped with **1** and **2** are much higher than those in thin films doped with **3**. This can be attributed to the incorporation of methyl groups in the central phenyl unit that rigidifies the molecular structure, yielding a



**Figure 3.** Normalized PL spectra of thin films of (a) **1**, (b) **2**, and (c) **3** doped into MCP at different concentrations (wt %) at 298 K.

high PLQY of up to 75%. In addition, all complexes show high decomposition temperatures of >300 °C.

**Electrochemistry.** The cyclic voltammetry of **1–3** in dichloromethane ( $0.1 \text{ mol dm}^{-3} \text{ } ^n\text{Bu}_4\text{NPF}_6$ ) has been investigated. In general, a quasi-reversible reduction couple at  $-1.32 \text{ V}$  vs saturated calomel electrode (SCE), and an irreversible oxidation wave at  $+0.90$ ,  $+0.90$ , and  $+0.83 \text{ V}$  vs SCE are found for **1–3**, respectively. The electrochemical data of **1–3** are summarized in Table 2, and the representative cyclic voltammograms are shown in Figure 5. The reduction process is assigned as the ligand-centered reduction. Compared with the unsubstituted diarylpyridine ligand,<sup>10</sup> an observation of a less negative reduction potential is due to the presence of the lower-lying  $\pi^*$  orbital associated with the difluorophenyl substituent on  $2,5\text{-F}_2\text{C}_6\text{H}_3\text{-C}^{\wedge}\text{N}^{\wedge}\text{C}$  ligand. While the first

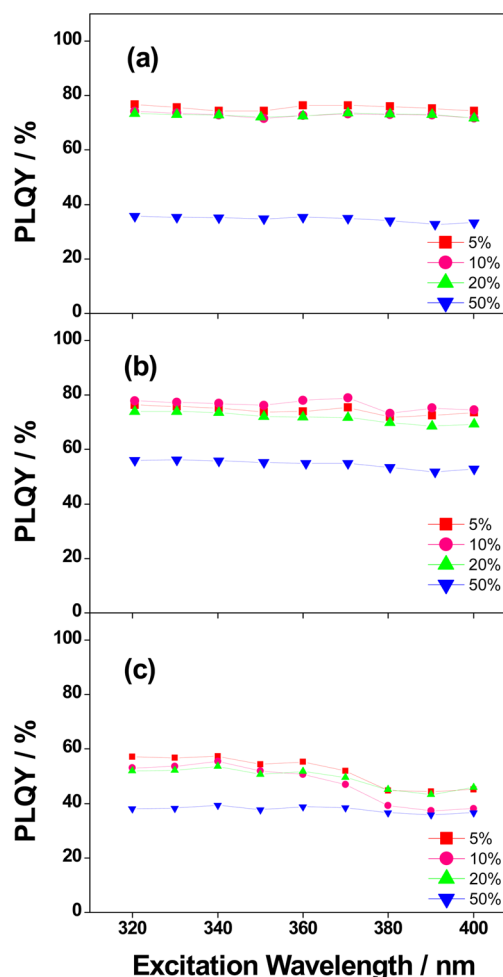


**Figure 4.** Absolute PLQY of (a) **1**, (b) **2**, and (c) **3** in MCP thin films.

oxidation wave of **1–3** is attributed to the alkynyl ligand-centered oxidation,<sup>10b,d,e,g,11</sup> the slight difference in the

**Table 1. Photophysical Properties of Complexes 1–3**

complex	absorption, $\lambda_{\text{max}}$ nm ( $\lambda_{\text{max}}$ $\text{dm}^3 \text{ mol}^{-1} \text{ cm}^{-1}$ )	medium ( $T$ , K)	emission, $\lambda_{\text{max}}$ nm ( $\tau_o$ , $\mu\text{s}$ )	$\Phi_{\text{PL}}(\text{soln})^a$	$\Phi_{\text{PL}}(\text{film})^b$
<b>1</b>	350 (48240), 390 (11390), 410 (7235)	$\text{CH}_2\text{Cl}_2$ (298)	697 (<0.1)	$3 \times 10^{-3}$	
		glass (77) <sup>c</sup> thin film (298)	528, 558 (120)		
		5% in MCP	524		0.77
		10% in MCP	527		0.74
		20% in MCP	540		0.73
		50% in MCP	562		0.36
<b>2</b>	320 (67580), 390 (8325), 410 (8470)	$\text{CH}_2\text{Cl}_2$ (298)	699 (<0.1)	$3 \times 10^{-2}$	
		glass (77) <sup>c</sup> thin film (298)	516, 546 (120)		
		5% in MCP	528		0.76
		10% in MCP	534		0.78
		20% in MCP	546		0.74
		50% in MCP	562		0.56
<b>3</b>	300 (54050), 330 (64500), 390 (4740), 410 (5850)	$\text{CH}_2\text{Cl}_2$ (298)	695 (<0.1)	$3 \times 10^{-3}$	
		glass (77) <sup>c</sup> thin film (298)	555 (70.6, 314.1) <sup>d</sup>		
		5% in MCP	530		0.57
		10% in MCP	536		0.53
		20% in MCP	548		0.52
		50% in MCP	570		0.38

<sup>a</sup>The luminescence quantum yield measured at room temperature using  $[\text{Ru}(\text{bpy})_3]\text{Cl}_2$  in aqueous solution as the reference (excitation wavelength = 436 nm,  $\Phi_{\text{lum}} = 0.042$ ). <sup>b</sup>Absolute  $\Phi_{\text{PL}}(\text{film})$  of **1–3** doped into MCP measured using 320 nm as the excitation wavelength. <sup>c</sup>Measured in EtOH–MeOH– $\text{CH}_2\text{Cl}_2$  (40:10:1, v/v). <sup>d</sup>Biexponential decay.

Table 2. Electrochemical Data for 1–3<sup>a</sup>

complex	oxidation, $E_{1/2}$ , V vs SCE <sup>b</sup> [ $E_{pa}$ , V vs SCE <sup>c</sup> ]	reduction $E_{1/2}$ , V vs SCE	$E_{HOMO}$ , eV <sup>d</sup>	$E_{LUMO}$ , eV <sup>d</sup>
1	[+0.90]	-1.32	-5.70	-3.48
2	[+0.90]	-1.32	-5.70	-3.48
3	[+0.83], +1.09	-1.32	-5.63	-3.48

<sup>a</sup>In CH<sub>2</sub>Cl<sub>2</sub> solution with 0.1 M <sup>n</sup>Bu<sub>4</sub>NPF<sub>6</sub> (TBAH) as supporting electrolyte at 298 K; working electrode, glassy carbon; scan rate = 100 mV s<sup>-1</sup>. <sup>b</sup> $E_{1/2} = (E_{pa} + E_{pc})/2$ ;  $E_{pa}$  and  $E_{pc}$  are the peak anodic and peak cathodic potentials, respectively. <sup>c</sup> $E_{pa}$  refers to the anodic peak potential for the irreversible oxidation wave. <sup>d</sup> $E_{HOMO}$  and  $E_{LUMO}$  levels were calculated from the first electrochemical potentials, that is,  $E_{HOMO} = -e(4.8 \text{ V} + E_{pa}^{ox})$ ;  $E_{LUMO} = -e(4.8 \text{ V} + E_{1/2}^{red})$ .

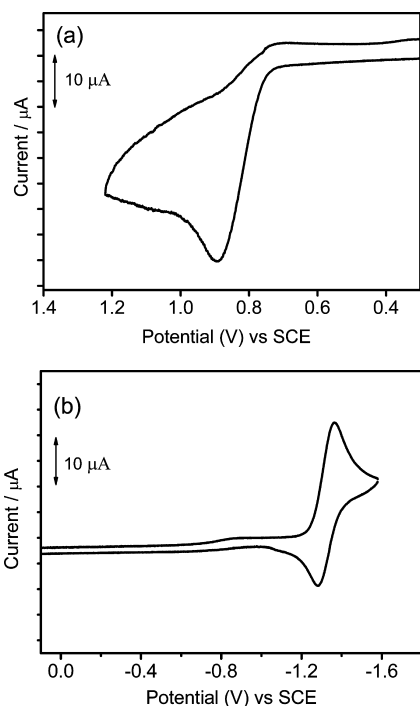


Figure 5. Cyclic voltammograms for the (a) oxidation and (b) reduction scans of 2 in CH<sub>2</sub>Cl<sub>2</sub> (0.1 M <sup>n</sup>Bu<sub>4</sub>NPF<sub>6</sub>).

potentials could be due to the presence of the electron-donating carbazolyl group on complex 3, and this in turn would lead to a destabilization of the highest occupied molecular orbital (HOMO) and thus a narrower HOMO–lowest unoccupied molecular orbital (LUMO) energy gap for 3.

**Electroluminescence Properties.** Solution-processable PHOLEDs based on bipolar alkynylgold(III) complexes as phosphorescent dopants have been prepared. PHOLEDs with the configuration of indium tin oxide (ITO)/poly(ethylenedioxythiophene):poly(styrene sulfonic acid) (PEDOT:PSS; 70 nm)/x % Au(III):MCP (60 nm)/tris(2,4,6-trimethyl-3-(pyridin-3-yl)phenyl)borane (3TPYMB; 5 nm)/1,3,5-tri[(3-pyridyl)phen-3-yl]benzene (TmPyPB; 30 nm)/LiF (0.8 nm)/Al (100 nm) are fabricated. 3TPYMB and TmPyPB are used as the hole-blocking and electron-transporting layers, respectively. The emissive layer is prepared by spin-coating a solution of Au(III):MCP blend at different concentrations in dichloromethane. Figure 6 depicts the EQE of devices doped with complexes 1–3 at different concentrations. As previously reported, the optimized device doped with carbazole-based alkynylgold(III) complex 3 (i.e., 20%) gives a high current

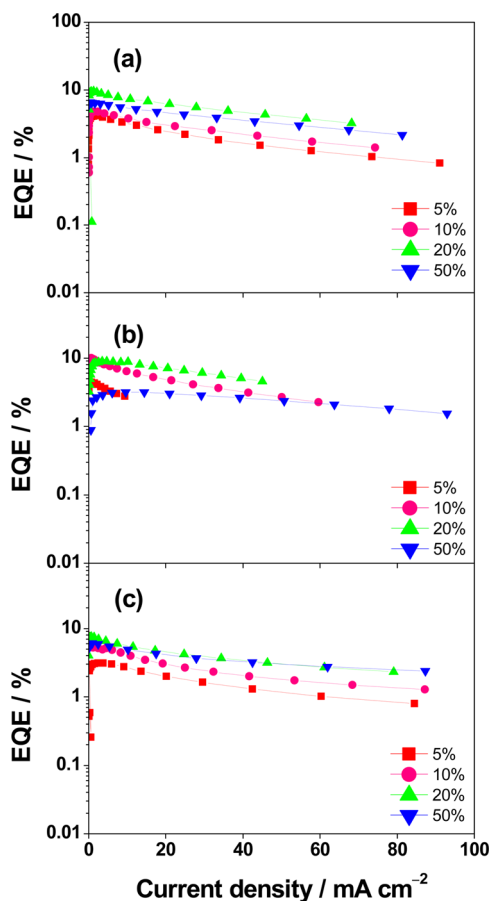


Figure 6. EQE of devices doped with complexes of (a) 1, (b) 2, and (c) 3 at different concentrations.

efficiency of 24.0 cd A<sup>-1</sup> and a power efficiency of 14.5 lm W<sup>-1</sup>.<sup>10b</sup> These values correspond to a maximum EQE of 7.8% at a current density of 0.1 mA cm<sup>-2</sup>. The incorporation of benzimidazole moieties can further enhance the EL performance. Particularly, the optimized devices doped with 1 (i.e., 20%) and 2 (i.e., 10%) show maximum current efficiencies of 30.4 and 33.6 cd A<sup>-1</sup>, respectively, corresponding to maximum EQEs of 9.5% and 10.0%. The discrepancies on device efficiencies between 1 and 2 can be ascribed to the higher PLQY in thin films doped with complex 2. On the other hand, compared with that of the device with 3, the dramatic improvement of EQEs is believed to be due to the bipolar character of the alkynylgold(III) complexes. Key parameters are summarized in Table 3. To evaluate the charge-transporting properties of 1 and 2, hole-only devices with structure of ITO/PEDOT:PSS/20% Au(III):MCP/MoO<sub>3</sub>/Al and electron-only devices with structure of ITO/LiF/20% Au(III):MCP/LiF/Al have been fabricated. MoO<sub>3</sub> and LiF layers are used to prevent electron- and hole-injection from the cathode and anode, respectively. For the hole-only devices, it is found that the current densities of all the devices are comparable (see Figure 7). This implies that the hole-transporting properties of all alkynylgold(III) complexes are similar. In contrast, the current densities of devices doped with bipolar complexes are much higher than that of the device doped with a carbazole-based complex, indicating that the incorporation of benzimidazole moieties can improve the electron-transporting properties of the alkynylgold(III) complexes.

Table 3. Key Parameters of Devices Fabricated with 1–3

complex	dopant concn, wt %	current efficiency, cd A <sup>-1</sup>	power efficiency, lm W <sup>-1</sup>	EQE, %	$\lambda_{\text{max}}$ , nm (CIE (x, y)) <sup>a</sup>
1	5	12.8	3.2	4.1	520 (0.30, 0.56)
	10	14.8	4.1	4.8	520 (0.31, 0.56)
	20	30.4	12.9	9.5	540 (0.38, 0.57)
2	5	19.6	13.5	6.6	564 (0.46, 0.53)
	5	14.1	3.4	4.4	520 (0.30, 0.56)
	10	33.6	8.7	10.0	532 (0.34, 0.58)
3	20	29.5	6.7	8.9	552 (0.41, 0.56)
	50	9.9	3.4	3.1	556 (0.44, 0.54)
	5	9.6	3.6	3.1	540 (0.37, 0.54)
3	10	24.0	14.5	7.8	548 (0.40, 0.54)
	20	22.7	17.7	7.6	560 (0.43, 0.53)
	50	15.6	13.8	6.1	580 (0.50, 0.49)

<sup>a</sup>Data were collected at a current density of 20 mA cm<sup>-2</sup>.

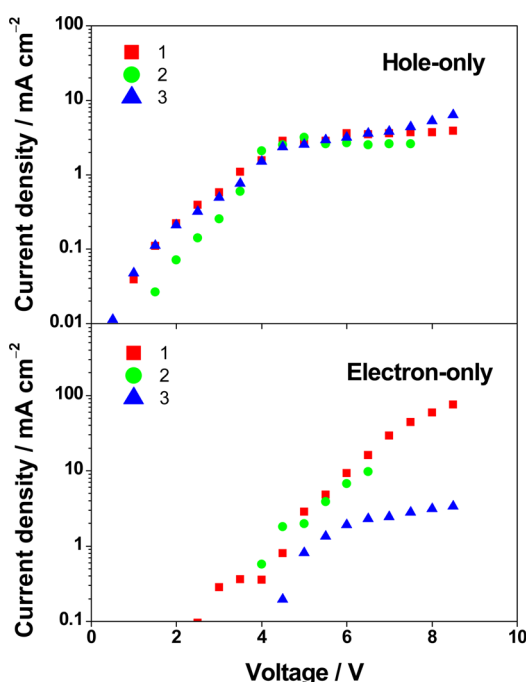


Figure 7. Current density–voltage curves of hole- and electron-only devices doped with alkynylgold(III) complexes 1–3.

Surprisingly, PHOLEDs with bipolar alkynylgold(III) complexes show a very small efficiency roll-off at practical brightness levels. For instance, at dopant concentration of 20%, the EQEs of devices doped with **1** remain as high as 8.8% and 5.4% at a luminance of 1000 and 5000 cd m<sup>-2</sup>, respectively (corresponding to EQE roll-off values of 7% and 43%, respectively). Remarkably, devices doped with **2** show an even smaller EQE roll-off. The EQE roll-off values are less than 1% and 21% at a luminance of 1000 and 5000 cd m<sup>-2</sup>, respectively. This is not the case for devices doped with **3**, where a poor performance with large EQE roll-offs of 16% at L = 1000 cd m<sup>-2</sup> and 65% at L = 5000 cd m<sup>-2</sup> are observed. As aforementioned, the change of formulation from chloroform to toluene can boost up the EQE to 10.1% for the device with **3** (see Figure 8). However, a severe EQE roll-off is also observed, in which the EQE drops by 14% at L = 1000 cd m<sup>-2</sup>. Table 4 summarizes the EL data of devices doped with 20% complexes 1–3. It should be mentioned that the EQEs of the present

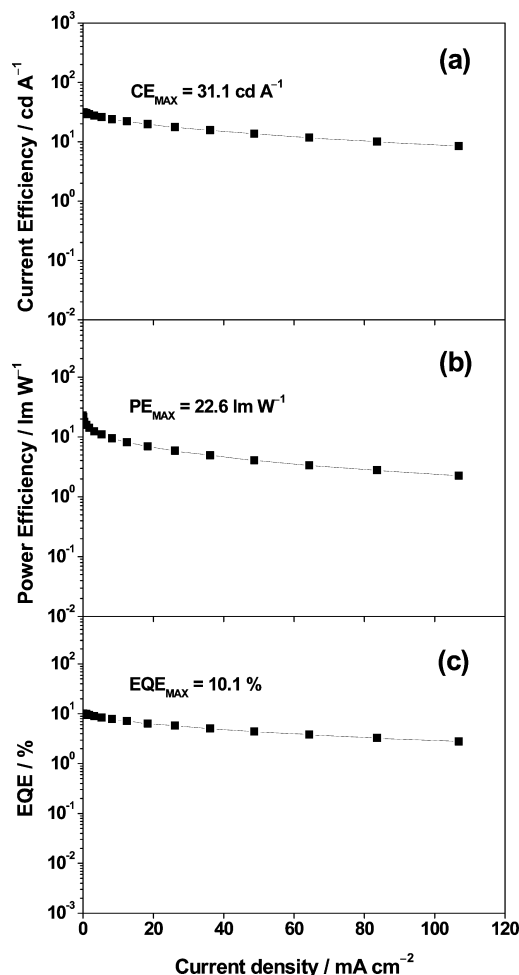


Figure 8. (a) Current efficiency (CE), (b) power efficiency (PE), and (c) EQE of device doped with 20% **3** in toluene.

Table 4. EL Data of Devices Doped with Complexes 1–3 (20%)

complex	max current efficiency, cd A <sup>-1</sup>	max power efficiency, lm W <sup>-1</sup>	EQE, % (EQE roll-off, %)		
			max	@1000 cd m <sup>-2</sup>	@5000 cd m <sup>-2</sup>
1	30.4	12.9	9.5	8.8 (7)	5.4 (43)
2	29.5	6.7	8.9	8.8 (1)	7.0 (21)
3	22.7	17.7	7.6	6.4 (16)	2.7 (65)

devices based on bipolar alkynylgold(III) complexes are among the highest for PHOLEDs based on bipolar transition metal complexes as well as other solution-processable PHOLEDs based on fluorene-containing cyclometalated gold(III) complexes.<sup>16</sup> In addition, the EQE roll-offs of the present devices are much smaller than that of the best solution-processable PHOLEDs based on the fluorene-containing cyclometalated gold(III) complexes as phosphorescent dopants reported recently (i.e., EQE roll-off of 91.7% at L = 1000 cd m<sup>-2</sup>).<sup>16</sup> The performance improvement may be rationalized in terms of the shorter emission lifetime as well as a better charge carrier balance of the present bipolar alkynylgold(III) complexes. Particularly, the emission lifetime of bipolar complexes are less than 0.1 μs, while those of the fluorene-containing alkynylgold(III) complexes are considerably longer (>170 μs).<sup>16</sup> Such long excited state lifetime would definitely lead to the accumulation

of triplet excitons within the emissive layer and hence results in severe T-T annihilation. These findings clearly demonstrate that the present bipolar alkynylgold(III) complexes are potential candidates as phosphorescent dopants for solution-processable PHOLEDs.

## CONCLUSION

A new class of bipolar alkynylgold(III) complexes containing triphenylamine and benzimidazole moieties has been successfully prepared. The incorporation of electron-accepting benzimidazole moiety can effectively enhance the electron-transporting properties of these gold(III) complexes as well as the PLQY in thin films. More importantly, highly efficient solution-processable PHOLEDs with EQE of up to 10.0% can be realized; particularly, the optimized devices demonstrate superior EL performance with small EQE roll-off values of less than 1% and 21% at practical brightness level of 1000 and 5000 cd m<sup>-2</sup>, respectively.

## EXPERIMENTAL SECTION

**Material and Reagents.** Triphenylamine was purchased by Acros Organics. All solvents were purified and distilled using standard procedures before use. All other reagents were of analytical grade and were used as received. Tetra-*n*-butylammonium hexafluorophosphate (Aldrich, 98%) was recrystallized for no less than three times from hot absolute ethanol prior to use.

**Synthesis of Precursor Ligands, L1 and L2.**  $\{(CH_3)_2CH\}_3Si-C\equiv C-TPA-(Me-DPBI)_2$ . To a well degassed solution of  $\{(CH_3)_2CH\}_3Si-C\equiv C-C_6H_4N(C_6H_4Br)_2$  (1.78 g, 3.05 mmol), 4-(1-phenyl-1*H*-benzimidazol-2-yl)phenylboronic acid (2.5 g, 6.10 mmol), and 2 M K<sub>2</sub>CO<sub>3</sub> (10 mL, 20 mmol) in toluene (40 mL) was added tetrakis(triphenylphosphine) palladium (208 mg, 0.16 mmol). The resulting mixture was stirred and heated to reflux at 120 °C for 24 h. To the mixture was then added deionized water (20 mL). The organic phase was separated, washed with brine solution three times, and then extracted three times with toluene. The organic extract was dried over anhydrous Na<sub>2</sub>SO<sub>4</sub> and filtered. Further purification was done by column chromatography (70–230 mesh) using hexane–ethyl acetate (6:1, v/v) as eluent. Subsequent recrystallization by diffusion of diethyl ether vapor into a concentrated solution of the product gave  $\{(CH_3)_2CH\}_3Si-C\equiv C-TPA-(Me-DPBI)_2$  as a pale yellow solid. Yield: 300 mg, 33%. <sup>1</sup>H NMR (300 MHz, acetone-*d*<sub>6</sub>, 298 K): δ 1.23 (s, 21H, –Si{CH(CH<sub>3</sub>)<sub>2</sub>}), 2.28 (s, 6H, methyl protons of Me-DPBI), 7.09 (d, *J* = 8.4 Hz, 2H, aryl protons of Me-DPBI), 7.20–7.36 (m, 16H, aryl protons of Me-DPBI and –NAr), 7.39–7.44 (m, 4H, aryl protons of Me-DPBI), 7.48 (d, *J* = 6.4 Hz, 4H, –NAr), 7.56–7.65 (m, 8H, aryl protons of Me-DPBI), 7.77 (d, *J* = 7.8 Hz, 2H, aryl protons of Me-DPBI). Positive FAB-MS: *m/z* 990 [M]<sup>+</sup>. Elemental Anal. Found (%): C, 81.17; H, 7.32; N, 5.59. Calcd for C<sub>69</sub>H<sub>63</sub>N<sub>5</sub>Si: C, 81.26; H, 7.25; N, 5.89.

$\{(CH_3)_2CH\}_3Si-C\equiv C-C_6H_4N(C_6H_3-Me-3)-(Me-DPBI)_2$ . This was synthesized by a procedure similar to that of  $\{(CH_3)_2CH\}_3Si-C\equiv C-TPA-(Me-DPBI)_2$  except that 2-methyl-4-(1-phenyl-1*H*-benzimidazol-2-yl)phenylboronic acid (1.2 g, 1.97 mmol) was used in place of 4-(1-phenyl-1*H*-benzimidazol-2-yl)phenylboronic acid. A pale yellow solid of  $\{(CH_3)_2CH\}_3Si-C\equiv C-C_6H_4N(C_6H_3-Me-3)-(Me-DPBI)_2$  was obtained. Yield: 400 mg, 21%. <sup>1</sup>H NMR (400 MHz, CDCl<sub>3</sub>, 298 K, relative to Me<sub>4</sub>Si): δ 1.12 (s, 21H, –Si{CH(CH<sub>3</sub>)<sub>2</sub>}), 1.94 (s, 6H, methyl protons of –C<sub>6</sub>H<sub>3</sub>-Me), 2.07 (s, 6H, methyl protons of Me-DPBI), 6.95–7.04 (m, 10H, aryl protons of Me-DPBI and –NAr), 7.22–7.39 (m, 14H, aryl protons of Me-DPBI and –NAr), 7.49–7.54 (m, 6H, aryl protons of Me-DPBI), 7.67 (s, 2H, aryl protons of Me-DPBI), 7.90 (d, *J* = 7.8 Hz, 2H, aryl protons of Me-DPBI). Positive FAB-MS: *m/z* 1017 [M]<sup>+</sup>. Elemental Anal. Found (%): C, 81.64; H, 7.00; N, 6.39. Calcd for C<sub>71</sub>H<sub>67</sub>N<sub>5</sub>Si·1/2H<sub>2</sub>O: C, 81.57; H, 6.74; N, 6.69.

**Ligand L1.** To a solution of  $\{(CH_3)_2CH\}_3Si-C\equiv C-TPA-(Me-DPBI)_2$  (180 mg, 0.18 mmol) and tetrahydrofuran (30 mL) was added a solution of tetra-*n*-butylammonium fluoride (0.1 M) in THF (1.2 mL). The solution was stirred for 4 h under nitrogen, and the solvent was removed. The residue was purified by column chromatography on silica gel (70–230 mesh) using hexane–acetone (20:1, v/v) as the eluent to give L1 as a pale white solid. Yield: 120 mg, 79%. <sup>1</sup>H NMR (300 MHz, CDCl<sub>3</sub>, 298 K, relative to Me<sub>4</sub>Si): δ 2.30 (s, 6H, methyl protons of Me-DPBI), 3.05 (s, 1H, –C≡CH), 7.07 (d, *J* = 8.4 Hz, 2H, aryl protons of Me-DPBI), 7.16–7.20 (m, 6H, aryl protons of Me-DPBI and –NAr), 7.25–7.30 (m, 10H, aryl protons of Me-DPBI and –NAr), 7.34–7.39 (m, 8H, aryl protons of Me-DPBI and –NAr), 7.47–7.56 (m, 6H, aryl protons of Me-DPBI), 7.68 (s, 2H, aryl protons of Me-DPBI), 7.90 (d, *J* = 7.8 Hz, 2H, aryl protons of Me-DPBI). Positive FAB-MS: *m/z* 834 [M]<sup>+</sup>. Elemental Anal. Found (%): C, 81.12; H, 6.22; N, 6.71. Calcd for C<sub>60</sub>H<sub>43</sub>N<sub>5</sub>: C, 80.94; H, 6.52; N, 6.68.

**Ligand L2.** This was synthesized by a procedure similar to that of L1 except that  $\{(CH_3)_2CH\}_3Si-C\equiv C-C_6H_4N(C_6H_3-Me-3)-(Me-DPBI)_2$  (500 mg, 0.20 mmol) was used in place of  $\{(CH_3)_2CH\}_3Si-C\equiv C-TPA-(Me-DPBI)_2$ . A pale yellow solid of L2 was obtained. Yield: 350 mg, 80%. <sup>1</sup>H NMR (400 MHz, CD<sub>2</sub>Cl<sub>2</sub>, 298 K, relative to Me<sub>4</sub>Si): δ 1.96 (s, 6H, methyl protons of –C<sub>6</sub>H<sub>3</sub>-Me), 2.09 (s, 6H, methyl protons of Me-DPBI), 3.05 (s, 1H, –C≡CH), 7.00–7.08 (m, 10H, aryl protons of Me-DPBI and –NAr), 7.29–7.42 (m, 14H, aryl protons of Me-DPBI and –NAr), 7.52–7.59 (m, 6H, aryl protons of Me-DPBI), 7.65 (s, 2H, aryl protons of Me-DPBI), 7.85 (d, *J* = 7.8 Hz, 2H, aryl protons of Me-DPBI). Positive FAB-MS: *m/z* 861 [M]<sup>+</sup>. Elemental Anal. Found (%): C, 84.65; H, 5.86; N, 7.73. Calcd for C<sub>62</sub>H<sub>47</sub>N<sub>5</sub>·H<sub>2</sub>O: C, 84.61; H, 5.61; N, 7.95.

**Synthesis of Alkynylgold(III) complexes.** All reactions were carried out under anaerobic and anhydrous conditions using standard Schlenk techniques.

$[Au\{2,5-F_2C_6H_3-C\equiv C-C\equiv C-TPA-(Me-DPBI)_2\}]$  (1). This was synthesized according to a modification of a literature procedure for bis(cyclometalated) diarylpyridine alkynylgold(III) complexes previously reported by us.<sup>10c–g</sup> A mixture of  $[Au\{2,5-F_2C_6H_3-C\equiv C\}Cl]$  (48 mg, 0.08 mmol), copper(I) iodide (2.0 mg, 0.01 mmol), triethylamine (2 mL), and L1 (80 mg, 0.09 mmol) in degassed dichloromethane (30 mL) solution was stirred at room temperature for 4 h. After removal of the solvent, the crude product was purified by column chromatography on silica gel using dichloromethane as the eluent. Subsequent recrystallization by diffusion of diethyl ether vapor into a concentrated solution of the product gave 1 as a pale yellow solid. Yield: 70 mg, 68%. <sup>1</sup>H NMR (500 MHz, CD<sub>2</sub>Cl<sub>2</sub>, 298 K, relative to Me<sub>4</sub>Si): δ 2.37 (s, 6H, methyl protons of Me-DPBI), 7.09 (d, *J* = 8.4 Hz, 2H, aryl protons of Me-DPBI), 7.14 (d, *J* = 8.4 Hz, 4H, –NAr), 7.17–7.21 (m, 4H, aryl protons of Me-DPBI and –NAr), 7.26–7.35 (m, 13H, aryl protons of Me-DPBI, –NAr and 2,5-F<sub>2</sub>C<sub>6</sub>H<sub>3</sub>– and –C<sub>6</sub>H<sub>4</sub>– of C<sup>^N^A^C</sup>), 7.43 (t, *J* = 7.2 Hz, 2H, –C<sub>6</sub>H<sub>4</sub>– of C<sup>^N^A^C</sup>), 7.42–7.63 (m, 16H, aryl protons of Me-DPBI), 7.79 (d, *J* = 7.8 Hz, 2H, aryl protons of Me-DPBI), 7.92 (d, *J* = 7.4 Hz, 2H, –C<sub>6</sub>H<sub>4</sub>– of C<sup>^N^A^C</sup>), 8.02 (d, *J* = 7.4 Hz, 2H, –C<sub>6</sub>H<sub>4</sub>– of C<sup>^N^A^C</sup>), 8.18 (s, 2H, pyridyl of C<sup>^N^A^C</sup>). Positive FAB-MS: *m/z* 1370 [M]<sup>+</sup>. IR (KBr disk): 2144 cm<sup>-1</sup> ν(C≡C). Elemental Anal. Found (%): C, 70.98; H, 4.06; N, 6.02. Calcd for C<sub>83</sub>H<sub>55</sub>N<sub>6</sub>F<sub>2</sub>Au·2H<sub>2</sub>O: C, 70.83; H, 4.22; N, 5.97.

$[Au\{2,5-F_2C_6H_3-C\equiv C-C\equiv C-C_6H_4N(C_6H_3-Me-3)-(Me-DPBI)_2\}]$  (2). This was synthesized by a procedure similar to that of complex 1 except that L2 (137 mg, 0.15 mmol) was used in place of L1. A yellow solid of 2 was obtained. Yield: 110 mg, 51%. <sup>1</sup>H NMR (500 MHz, CD<sub>2</sub>Cl<sub>2</sub>, 298 K, relative to Me<sub>4</sub>Si): δ 1.98 (s, 6H, methyl protons of –C<sub>6</sub>H<sub>3</sub>-Me), 2.09 (s, 6H, methyl protons of Me-DPBI), 7.01 (s, 4H, aryl protons of Me-DPBI), 7.05–7.11 (m, 6H, –NAr), 7.23–7.48 (m, 19H, aryl protons of Me-DPBI, –NAr and 2,5-F<sub>2</sub>C<sub>6</sub>H<sub>3</sub>– and –C<sub>6</sub>H<sub>4</sub>– of C<sup>^N^A^C</sup>), 7.52–7.58 (m, 8H, aryl protons of Me-DPBI and –NAr), 7.68 (s, 2H, aryl protons of Me-DPBI), 7.66–7.72 (m, 4H, pyridyl and –C<sub>6</sub>H<sub>4</sub>– of C<sup>^N^A^C</sup>), 7.92 (d, *J* = 7.4 Hz, 2H, aryl protons of Me-DPBI), 8.02 (d, *J* = 7.4 Hz, 2H, –C<sub>6</sub>H<sub>4</sub>– of C<sup>^N^A^C</sup>). Positive FAB-MS: *m/z* 1372 [M]<sup>+</sup>. IR (KBr disk): 2148 cm<sup>-1</sup> ν(C≡C). Elemental

Anal. Found (%): C, 72.57; H, 4.61; N, 5.86. Calcd for  $C_{88}H_{59}N_6F_2Au-1/2H_2O$ : C, 72.48; H, 4.30; N, 5.96.

**Physical Measurements and OLED Fabrication.** All physical measurements and instrumentation for the characterization of the identities and photophysical properties of the alkynylgold(III) complexes were the same as described in our previous works.<sup>11</sup> For OLED fabrication, devices with the structure of ITO/PEDOT:PSS (70 nm)/emissive layer (60 nm)/3TPyMB (5 nm)/TmPyPB (30 nm)/LiF (0.8 nm)/Al (100 nm) were fabricated, in which the emissive layer was formed by mixing the dendrimer with MCP to prepare a 10 mg  $cm^{-3}$  solution in chloroform via spin-coating technique. Experimental procedures for fabrication and characterization of OLEDs were described in detail elsewhere.<sup>10b-e</sup>

## AUTHOR INFORMATION

### Corresponding Authors

wwym@hku.hk  
chanmym@hku.hk

### Present Address

†K.M.-C.W.: Department of Chemistry, South University of Science and Technology of China, Shenzhen, P. R. China.

### Notes

The authors declare no competing financial interest.

## ACKNOWLEDGMENTS

V.W.-W.Y. acknowledges support from The University of Hong Kong and the URC Strategic Research Theme on New Materials. The work described in this paper was fully supported by a grant from the Theme-Based Research Scheme of the Research Grants Council of the Hong Kong Special Administrative Region, China (Project No. T23-713/11). M.-C.T. and Y.-C.W. acknowledge the receipt of postgraduate studentships from The University of Hong Kong.

## REFERENCES

- (1) (a) Helander, M. G.; Wang, Z. B.; Qiu, J.; Greiner, M. T.; Puzzo, D. P.; Liu, Z. W.; Lu, Z. H. *Science* **2011**, *332*, 944. (b) Kim, S.-Y.; Jeong, W.-K.; Mayr, C.; Park, Y.-S.; Kim, K.-H.; Lee, J.-H.; Moon, C.-K.; Brütting, W.; Kim, J.-J. *Adv. Funct. Mater.* **2013**, *23*, 3896.
- (2) (a) Meerheim, R.; Walzer, K.; Pfeiffer, M.; Leo, K. *Appl. Phys. Lett.* **2006**, *89*, No. 061111. (b) He, G.; Rothe, S.; Murano, S.; Waerner, A.; Zeika, O.; Birstock, J. *J. Soc. Inf. Dispersion* **2009**, *17*, 159.
- (3) Murawski, C.; Leo, K.; Gather, M. C. *Adv. Mater.* **2013**, *25*, 6801.
- (4) (a) Kepler, R. G.; Caris, J. C.; Avakian, P.; Abramson, E. *Phys. Rev. Lett.* **1963**, *10*, 400. (b) Baldo, M. A.; Adachi, C.; Forrest, S. R. *Phys. Rev. B* **2000**, *62*, 10967. (c) Kim, S. H.; Jang, J.; Yook, K. S.; Lee, J. Y. *Appl. Phys. Lett.* **2008**, *92*, No. 023513.
- (5) (a) Tsutsui, T.; Yang, M.; Yahiro, M.; Nakamura, K.; Watanabe, T.; Tsuji, T.; Fukuda, Y.; Wakimoto, T.; Miyaguchi, S. *Jpn. J. Appl. Phys.* **1999**, *38*, 1502. (b) Baldo, M. A.; Lamansky, S.; Burrows, P. E.; Thompson, M. E.; Kwong, R. C. *Appl. Phys. Lett.* **1999**, *75*, 4. (c) Yan, D.; Han, L.; Li, W.; Chu, B.; Su, Z.; Zhang, D.; Li, T.; Zhang, G.; Zhu, J. *J. Phys. D: Appl. Phys.* **2010**, *43*, No. 10S101.
- (6) (a) Hecht, S.; J. Fréchet, M. J. *Angew. Chem., Int. Ed.* **2001**, *40*, 74. (b) Zhou, G.; Wong, W.-Y.; Yao, B.; Xie, Z.; Wang, L. *Angew. Chem., Int. Ed.* **2007**, *46*, 1149. (c) Burn, P. L.; Lo, S.-C.; Samuel, I. D. W. *Adv. Mater.* **2007**, *19*, 1675. (d) Qin, T.; Ding, J.; Wang, L.; Baumgarten, M.; Zhou, G.; Müllen, K. *J. Am. Chem. Soc.* **2009**, *131*, 14329. (e) Barron, J. A.; Bernhaed, S.; Houston, P. L.; Abruña, H. D.; Ruglovsky, J. L.; Malliaras, G. G. *J. Phys. Chem. A* **2003**, *107*, 8130. (f) Pu, Y.-J.; Harding, R. E.; Stevenson, S. G.; Namdas, E. B.; Tedeschi, C.; Markham, J. P. J.; Rummings, R. J.; Burn, P. L.; Samuel, I. D. W. *J. Mater. Chem.* **2007**, *17*, 4255.
- (7) (a) Erickson, N. C.; Holmes, R. J. *Appl. Phys. Lett.* **2010**, *97*, No. 083308. (b) Erickson, N. C.; Holmes, R. J. *Adv. Funct. Mater.*

**2013**, *23*, 5190. (c) Zhu, Y.; Kulkarni, P.; Wu, P.-T.; Jenekhe, S. A. *Chem. Mater.* **2008**, *20*, 4200.

(8) (a) Hung, M.-C.; Liao, J.-L.; Chen, S.-A.; Chen, S.-H.; Su, A.-C. *J. Am. Chem. Soc.* **2005**, *127*, 14576. (b) Hsu, F.-M.; Chien, C.-H.; Shih, P.-I.; Su, C.-F. *Chem. Mater.* **2009**, *21*, 1017. (c) Su, S.-J.; Cai, C.; Kido, J. *Chem. Mater.* **2010**, *23*, 274. (d) Gong, S.; Chen, Y.; Yang, C.; Zhong, C.; Qin, J.; Ma, D. *Adv. Mater.* **2010**, *22*, 5370. (e) Zhang, Y.; Zuniga, C.; Kim, S.-J.; Cai, D.; Barlow, S.; Salman, S.; Coropceanu, V.; Brédas, J.-L.; Kippelen, B.; Marder, S. *Chem. Mater.* **2011**, *23*, 4002. (f) Ge, Z.; Hayakawa, T.; Ando, S.; Ueda, M.; Akiike, T.; Miyamoto, H.; Kajita, T.; Kakimoto, M. *Adv. Funct. Mater.* **2008**, *18*, 584. (g) Jeon, S. O.; Jang, S. E.; Son, H. S.; Lee, J. Y. *Adv. Mater.* **2011**, *23*, 1436. (h) Tao, Y.; Wang, Q.; Ao, L.; Zhong, C.; Qin, J.; Yang, C.; Ma, D. *J. Mater. Chem.* **2010**, *20*, 1759.

(9) (a) He, Z.; Wong, W.-Y.; Yu, X.; Kwok, H.-S.; Lin, Z. *Inorg. Chem.* **2006**, *45*, 10922. (b) Chen, L.; Ding, J.; Cheng, Y.; Xie, Z.; Wang, L.; Jing, X.; Wang, F. *Chem.—Asian J.* **2011**, *6*, 1372. (c) Peng, T.; Li, G.; Ye, K.; Wang, C.; Zhao, S.; Liu, Y.; Hou, Z.; Wang, Y. *J. Mater. Chem. C* **2013**, *1*, 2920.

(10) (a) Yam, V. W.-W.; Choi, S. W.-K.; Lai, T.-F.; Lee, W.-L. *J. Chem. Soc., Dalton Trans.* **1993**, 1001. (b) Tang, M.-C.; Tsang, D. P.-K.; Chan, M. M.-Y.; Wong, K. M.-C.; Yam, V. W.-W. *Angew. Chem., Int. Ed.* **2013**, *52*, 446. (c) Wong, K. M.-C.; Zhu, X.; Hung, L.-L.; Zhu, N.; Yam, V. W.-W.; Kwok, H.-S. *Chem. Commun.* **2005**, 2906. (d) Au, V. K.-M.; Wong, K. M.-C.; Tsang, D. P.-K.; Chan, M.-Y.; Zhu, N.; Yam, V. W.-W. *J. Am. Chem. Soc.* **2010**, *132*, 14273. (e) Au, V. K.-M.; Tsang, D. P.-K.; Wong, K. M.-C.; Chan, M.-Y.; Zhu, N.; Yam, V. W.-W. *Inorg. Chem.* **2013**, *52*, 12713. (f) Yam, V. W.-W.; Wong, K. M.-C.; Hung, L.-L.; Zhu, N. *Angew. Chem., Int. Ed.* **2005**, *44*, 3107. Yam, V. W.-W.; Wong, K. M.-C.; Hung, L.-L.; Zhu, N. *Angew. Chem.* **2005**, *117*, 3167. (g) Wong, K. M.-C.; Hung, L.-L.; Lam, W. H.; Zhu, N.; Yam, V. W.-W. *J. Am. Chem. Soc.* **2007**, *129*, 4350. (h) Au, V. K.-M.; Lam, W. H.; Wong, W.-T.; Yam, V. W.-W. *Inorg. Chem.* **2012**, *51*, 7537. (i) Au, V. K.-M.; Wong, K. M.-C.; Zhu, N.; Yam, V. W.-W. *Chem.—Eur. J.* **2011**, *17*, 130. (j) Au, V. K.-M.; Zhu, N.; Yam, V. W.-W. *Inorg. Chem.* **2013**, *52*, 558.

(11) Tang, M. C.; Chan, C. K.-M.; Tsang, D. P.-K.; Wong, Y.-C.; Chan, M. M.-Y.; Wong, K. M.-C.; Yam, V. W.-W. *Chem.—Eur. J.* **2014**, *20*, 15233.

(12) (a) Mclroy, S. P.; Clo, E.; Nikolajsen, L.; Frederiksen, P. K.; Nielsen, C. B.; Mikkelsen, K. V.; Gøthelr, K. V.; Ogilby, P. R. *J. Org. Chem.* **2005**, *70*, 1134. (b) Onitsuka, K.; Ohara, N.; Takei; Takahashi, F. *S. Dalton Trans.* **2006**, 3693.

(13) Kröhnke, F. *Synthesis* **1976**, 1.

(14) Wong, K.-H.; Cheung, K.-K.; Chan, M. C.-W.; Che, C.-M. *Organometallics* **1998**, *17*, 3505.

(15) (a) Albrecht, K.; Yamamoto, K. *J. Am. Chem. Soc.* **2009**, *131*, 2244. (b) Ding, J.; Gao, J.; Cheng, Y.; Xie, Z.; Wang, L.; Ma, D.; Jing, X.; Wang, F. *Adv. Funct. Mater.* **2006**, *16*, 575. (c) Ding, J.; Lü, J.; Cheng, Y.; Xie, Z.; Wang, L.; Jing, X.; Wang, F. *Adv. Funct. Mater.* **2008**, *18*, 2754. (d) Ding, J.; Wang, B.; Yue, Z.; Yao, B.; Xie, Z.; Cheng, Y.; Wang, L.; Jing, X.; Wang, F. *Angew. Chem., Int. Ed.* **2009**, *48*, 6664.

(16) Cheng, G.; Chan, K. T.; To, W.-P.; Che, C.-M. *Adv. Mater.* **2014**, *26*, 2540.